Moment approach to the bootstrap current in nonaxisymmetric toroidal plasmas using δf Monte Carlo methods

A. Matsuyama,[1,a)] M. Yu. Isaev,[2] K. Y. Watanabe,[3] K. Hanatani,[4] Y. Suzuki,[3] N. Nakajima,[3] W. A. Cooper,[5] and T. M. Tran[5]

[1]*Graduate School of Energy Science, Kyoto University, Gokasho, Uji, Kyoto 611-0011, Japan*
[2]*Nuclear Fusion Institute, RRC Kurchatov Institute, 123182 Moscow, Russia*
[3]*National Institute for Fusion Science, Toki, Gifu 509-5292, Japan*
[4]*Institute of Advanced Energy, Kyoto University, Gokasho, Uji, Kyoto 611-0011, Japan*
[5]*Centre de Recherches en Physique des Plasmas, Association Euratom-Suisse,*
Ecole Polytechnique Fédérale de Lausanne, CH1015 Lausanne, Switzerland

To evaluate the bootstrap current in nonaxisymmetric toroidal plasmas quantitatively, a δf Monte Carlo method is incorporated into the moment approach. From the drift-kinetic equation with the pitch-angle scattering collision operator, the bootstrap current and neoclassical conductivity coefficients are calculated. The neoclassical viscosity is evaluated from these two monoenergetic transport coefficients. Numerical results obtained by the δf Monte Carlo method for a model heliotron are in reasonable agreement with asymptotic formulae and with the results obtained by the variational principle. © *2009 American Institute of Physics*. [DOI: 10.1063/1.3121223]

I. INTRODUCTION

The bootstrap current in nonaxisymmetric toroidal devices has significant influence on the confinement properties of a plasma, such as equilibrium and stability, through the change in rotational transform profiles and magnetic field spectra.[1–4] Because the bootstrap current is induced predominantly by the trapping and detrapping of particles in the low-collisionality regime,[5,6] a collision operator of the drift-kinetic equation can be modeled appropriately by the pitch-angle scattering term. With this assumption, a bootstrap current coefficient D_{31} has been calculated numerically for various nonaxisymmetric configurations.[7] This coefficient D_{31} is proportional to the geometric factor,[8] which characterizes the relative amplitude and sign of the bootstrap current for a given toroidal configuration. For example, the δf Monte Carlo method[9,10] constitutes an efficient numerical technique to calculate D_{31} by guiding-center particle simulations.

To evaluate the bootstrap current in a satisfactory manner, however, we also need to take into account the momentum conservation law of like-particle collisions and the coupling between electrons and ions. Consequently, the δf Monte Carlo method for D_{31}, which relies only on the pitch-angle scattering operator, is inadequate to evaluate the bootstrap current quantitatively. In the analytical theory by Shaing and Callen,[8] the bootstrap current $\langle J_\parallel B \rangle$ on each flux surface is determined from the momentum and heat-flux balance equations along the field lines. To treat such macroscopic balances correctly, one must simulate ensembles of test electrons and ions with Maxwellian distributions and to use the like and unlike-particle collision operators that preserve the conservation laws. To date, such a self-consistent Monte Carlo simulation of the bootstrap current has been

reported only for tokamaks[11] but not for nonaxisymmetric devices.

Recently, Sugama and Nishimura[12,13] developed another method to evaluate the bootstrap current, which overcomes the above difficulties. They showed that parallel viscosities $\langle \mathbf{B} \cdot (\nabla \cdot \boldsymbol{\pi}_a) \rangle$ and $\langle \mathbf{B} \cdot (\nabla \cdot \boldsymbol{\Theta}_a) \rangle$ can be evaluated numerically using the drift-kinetic equation solver (DKES) code;[14,15] substituting these viscosity terms into the moment equations,[16] the bootstrap current is determined algebraically without breaking the conservation laws. While based on the pitch-angle scattering approximation, the important feature of the DKES code is that *all* the elements of the monoenergetic transport matrix D_{ij} $(i, j = 1, 3)$ can be calculated by the variational principle. We emphasize that this moment approach takes computational advantages of the pitch-angle scattering operator and yet satisfies the physical requirement of the conservation laws of the linearized Fokker–Planck collision operator.[12,17]

In the moment approach by Sugama and Nishimura, not only the nondiagonal element D_{31} but also the diagonal one D_{33} of the monoenergetic transport matrix is required to calculate the neoclassical viscosity. To our knowledge, D_{33}, which corresponds to a (monoenergetic) neoclassical conductivity coefficient, has been calculated so far only by the DKES code. We mention that this diagonal term D_{33} can be related to the damping rate of neoclassical flows along the field lines and is indispensable to determine the neoclassical viscosity. Considering the δf Monte Carlo method for D_{31}, an extension of the method to the calculation of D_{33} will be useful to evaluate the bootstrap current quantitatively with the moment approach.

The purpose of this paper is twofold: (i) to develop a δf Monte Carlo method that calculates the monoenergetic transport coefficient D_{33} and (ii) to incorporate this method into the moment approach for evaluating the bootstrap current $\langle J_\parallel B \rangle$. Following the moment approach for the DKES code,

a)Electronic mail: matuyama@center.iae.kyoto-u.ac.jp

the neoclassical parallel viscosities $\langle \mathbf{B} \cdot (\nabla \cdot \boldsymbol{\pi}_a) \rangle$ and $\langle \mathbf{B} \cdot (\nabla \cdot \boldsymbol{\Theta}_b) \rangle$ are obtained from an output of the δf Monte Carlo method, i.e., D_{31} and D_{33}. We have implemented the δf weighting scheme presented here into the VENUS+δf code[9] developed at CRPP (Switzerland). The numerical calculation of the neoclassical viscosities is tested for a magnetic-field model of the large helical device (LHD).[18]

This paper is organized as follows. In Sec. II, the moment approach to evaluate the bootstrap current using the δf Monte Carlo method is described. We begin with the drift-kinetic equation with the pitch-angle scattering approximation and derive a δf weighting scheme to calculate D_{31} and D_{33}. The evaluation of the bootstrap current from these transport coefficients is also discussed. In Sec. III, we describe the numerical procedure and show benchmarking results with asymptotic formulae and with the DKES code. Finally, the conclusion will be given in Sec. IV. In the Appendix, an additional topic on the present δf Monte Carlo method will be discussed.

II. MOMENT APPROACH WITH A δf MONTE CARLO METHOD

A. Basic formalism

We first consider the drift-kinetic theory based on the pitch-angle scattering approximation. In this paper, we use the coordinate system $(\mathbf{x}, v, \xi)$, where $\mathbf{x}$ is the guiding-center position, v is the particle velocity, and $\xi \equiv v_\parallel / v$ is the pitch variable. For transport applications, the guiding-center position is usually written in Boozer coordinates,[19] (s, θ, ζ): s is the surface label, θ is the poloidal angle, and ζ is the toroidal angle. The Jacobian of the Boozer coordinate is denoted by $\mathcal{J}_B$. The flux surface average in this coordinate is defined by $\langle A \rangle \equiv (\oint\oint d\theta d\zeta \mathcal{J}_B A)/(\oint\oint d\theta d\zeta \mathcal{J}_B)$.

The neoclassical transport coefficients are calculated from a steady-state solution of the linearized drift-kinetic equation. Let $f = f_0 + \delta f$, where

$$f_0 \equiv f_M = \frac{n(s)}{\pi^{3/2} v_T^3} \exp(-K) \tag{1}$$

is a local Maxwellian with the density $n(s)$ and the temperature $T(s)$ and δf is the perturbed part of a gyroaveraged distribution function; $v_T = (2T/m)^{1/2}$ is the local thermal velocity and $K = mv^2/2T$ is the normalized kinetic energy. Approximating a collision operator by the pitch-angle scattering term, the linearized drift-kinetic equation is written in terms of $g \equiv \delta f / f_0$ as

$$(V_\parallel - C)g = \mathbf{v}_d \cdot \nabla s A_1 + Bv\xi A_E, \tag{2}$$

where

$$V_\parallel = v\xi \mathbf{b} \cdot \nabla - \frac{1}{2}v(1-\xi^2)(\mathbf{b} \cdot \nabla \ln B)\frac{\partial}{\partial \xi}, \tag{3}$$

$$C = \frac{\nu_D}{2} \frac{\partial}{\partial \xi}(1-\xi^2)\frac{\partial}{\partial \xi}, \tag{4}$$

$$A_1 = -\frac{1}{n}\frac{\partial n}{\partial s} - \frac{e}{T}\frac{\partial \Phi}{\partial s}, \tag{5}$$

$$A_E = \frac{e}{T}\frac{\langle BE_\parallel \rangle}{\langle B^2 \rangle}. \tag{6}$$

Here, $B \equiv |\mathbf{B}|$ is the equilibrium magnetic-field strength, $\mathbf{b} \equiv \mathbf{B}/B$ is the unit vector along the field line, $E_\parallel$ is the parallel electric field, and Φ is the electrostatic potential. In Eq. (2), $\mathbf{v}_d$ denotes the guiding-center drift velocity, while in the left-hand side of Eq. (2) we explicitly assume the steady-state solution such that $\partial g / \partial t \equiv 0$. The pitch-angle scattering term C is characterized by the deflection frequency ν_D, and the operator $V_\parallel$ only includes terms up to the zeroth order of $\rho_p/a \ll 1$, where $\rho_p = mv/eB_p$ is the poloidal gyroradius (with the characteristic poloidal magnetic field B_p) and a is the plasma minor radius. Equation (2) is derived with the neoclassical ordering, i.e., $\rho_p/a \ll 1$, which means the radial orbit width is assumed to be small enough and the transport coefficients can be determined locally on a flux surface. The temperature gradient $\partial T / \partial s$ is also neglected here. The monoenergetic transport matrix $D_{ij}(K)$ $(i,j=1,3)$, which is a function of the normalized kinetic energy K or equivalently that of the collisionality ν_D/v, is defined in the DKES code[14,15] as follows:

$$D_{ij}(K) \equiv (\sigma_i^+, F_j^+) + (\sigma_i^+, F_j^-) \quad (i,j=1,3). \tag{7}$$

In the DKES code, the drift-kinetic equation [Eq. (2)] is separated in terms of the symmetric (+) and antisymmetric (−) parts of the distribution function $F_j^\pm$ $(j=1,3)$ with respect to the time-reversal operation such that

$$V_\parallel F_j^- - CF_j^+ = \sigma_j^+, \tag{8}$$

$$V_\parallel F_j^+ - CF_j^- = 0 \quad (j=1,3),$$

with

$$\sigma_1^+ = -\mathbf{v}_d \cdot \nabla s = -\frac{2v^2}{3\Omega}\left[1 + \frac{1}{2}P_2(\xi)\right]\mathbf{b} \times \nabla \ln B \cdot \nabla s, \tag{9}$$

$$\sigma_3^+ = V_\parallel(Bv\xi/\nu_D) = \frac{v^2}{\nu_D}P_2(\xi)\mathbf{B} \cdot \nabla \ln B. \tag{10}$$

Here, $\Omega = eB/m$ is the gyrofrequency and $P_2(\xi) \equiv (3\xi^2 - 1)/2$ denotes the second-order Legendre polynomial. The parentheses in Eq. (7) denote the inner-product operation defined by

$$(\alpha, \beta) = \frac{1}{2}\int_{-1}^{1} d\xi \langle \alpha\beta \rangle, \tag{11}$$

where $\langle \cdot \rangle$ denotes the flux surface average. Note that the time-reversal symmetric properties of the operators $V_\parallel$ and C with respect to this inner-product operation apply such that

$$(V_\parallel \alpha, \beta) = -(\alpha, V_\parallel \beta), \quad (C\alpha, \beta) = (\alpha, C\beta). \tag{12}$$

Equation (8) is derived with the adjoint equation[14,15] of the drift-kinetic equation, which prevents us from solving Eq. (8) by δf Monte Carlo methods. Hence we need to con-

struct an alternative set of the drift-kinetic equations that can be solved as an initial-value problem using guiding-center particle simulations. We now decompose the dependence of the perturbed distribution function g into two independent thermodynamic forces A_1 and A_E so that $g = g_1 A_1 + g_E A_E$, which yields

$$(V_\parallel - C)g_1 = -\sigma_1^+, \tag{13}$$

$$(V_\parallel - C)g_E = Bv\xi. \tag{14}$$

Comparing Eqs. (13) and (14) with Eq. (8), we have obtained the following relations:

$$g_1 = -(F_1^+ + F_1^-), \tag{15}$$

$$g_E = -(F_3^+ + F_3^-) + Bv\xi/\nu_D. \tag{16}$$

If we take the inner-product operation of $eBv\xi$ with the solutions of Eqs. (13) and (14), the current carried by test particles in a simulation, which is here denoted by $\hat{j} \equiv \hat{j}_{bs} + \hat{j}_{Oh}$, is explicitly written in terms of D_{31} and D_{33},

$$\hat{j}_{bs} \equiv e(Bv\xi, g_1)A_1 = -eD_{31}A_1, \tag{17}$$

$$\hat{j}_{Oh} \equiv e(Bv\xi, g_E)A_E = -eD_{33}A_E + \frac{e\langle B^2\rangle v^2}{3\nu_D}A_E, \tag{18}$$

where $\hat{j}_{bs}$ and $\hat{j}_{Oh}$ denote the monoenergetic bootstrap and Ohmic currents, respectively. Equation (17) allows us to calculate the bootstrap current coefficient D_{31} from the steady-state solution g_1. On the other hand, Eq. (18) yields the neoclassical conductivity coefficient D_{33}, but the inclusion of the second term in the right-hand side of Eq. (18) is unfavorable with respect to numerical accuracy. This term comes from the classical Spitzer distribution $g_S \equiv Bv\xi/\nu_D$, where g_S is the solution of the equation[15] such that $-Cg_S = Bv\xi$. To eliminate this Spitzer current from Eq. (18), we introduce the drift-kinetic equation such that

$$(V_\parallel - C)g_3 = -\sigma_3^+, \tag{19}$$

where

$$g_3 \equiv g_E - g_S = -(F_3^+ + F_3^-). \tag{20}$$

Using the steady-state solution of Eq. (19), we obtain the monoenergetic neoclassical-conductive current $\hat{j}_{nc}$ as

$$\hat{j}_{nc} \equiv e(Bv\xi, g_3)A_E = -eD_{33}A_E. \tag{21}$$

Equation (21) is more appropriate than Eq. (18) to calculate D_{33} because in the collisional regime, the classical Spitzer current $\hat{j}_{Sp} \equiv e\langle B^2\rangle v^2 A_E/(3\nu_D)$ dominates over the first term in Eq. (18) in the expression for $\hat{j}_{Oh}$. This prohibits the accurate evaluation of D_{33} using Eq. (18). As a result, we find that the monoenergetic transport coefficients D_{31} and D_{33} are calculated from the steady-state solution of the drift-kinetic equations [Eqs. (13) and (19)]. It should be noted that these equations are consistent with the DKES code through the explicit relations in Eqs. (15) and (20).

B. δf weighting scheme

Next, we develop a δf weighting scheme to solve the drift-kinetic equations of Eqs. (13) and (19). It is well known that the introduction of marker weights into Monte Carlo simulations reduces the statistical noise up to the order of $\delta f/f$. Here, to solve Eqs. (13) and (19) simultaneously, we introduce two marker weights $w_1 \equiv g_1/F_m$ and $w_3 \equiv g_3/F_m$, where $F_m(\mathbf{x}, \xi)$ denotes a distribution function of test particles. We note that the particle velocity v is now manifestly a constant of motion, i.e., $v = \text{const}$. These two marker weights, w_1 and w_3, are assigned to test particles and are updated by the integration along the test-particle trajectories. The time evolution of w_i is represented in terms of the Lagrangian derivative as

$$\frac{Dw_i}{Dt} = -\sigma_i^+ \quad (i = 1, 3). \tag{22}$$

For $i = 1$, the right-hand side of Eq. (22) corresponds to the radial excursion of test particles such that $\sigma_1^+ = -ds/dt$. The Lagrangian derivative D/Dt is given by

$$\frac{D}{Dt} \equiv \frac{\partial}{\partial t} + V_\parallel - C, \tag{23}$$

where the equilibrium trajectory defined by Eq. (23) can be simulated with the Monte Carlo method as will be described later. At each time step of the simulation, the monoenergetic transport coefficients D_{31} and D_{33} can be calculated by the δf Monte Carlo integral.[20] Using Eqs. (17) and (21), we obtain

$$D_{31} = -\frac{\sum_{n=1}^{N}\mathcal{J}_B(\mathbf{x}_n)B(\mathbf{x}_n)v\xi_n w_1^{(n)}}{\sum_{n=1}^{N}\mathcal{J}_B(\mathbf{x}_n)} \tag{24}$$

and

$$D_{33} = -\frac{\sum_{n=1}^{N}\mathcal{J}_B(\mathbf{x}_n)B(\mathbf{x}_n)v\xi_n w_3^{(n)}}{\sum_{n=1}^{N}\mathcal{J}_B(\mathbf{x}_n)}, \tag{25}$$

where N is the number of test particles. All the quantities in the right-hand sides in Eqs. (24) and (25) are given along the trajectory in $(\mathbf{x}, \xi)$ space. To derive Eqs. (24) and (25), we have used here that

$$g(\mathbf{x}, \xi) - g_S = \frac{1}{C_N}\sum_{n=1}^{N}\left[w_1^{(n)}\delta(\mathbf{x} - \mathbf{x}_n)\delta(\xi - \xi_n)A_1 \right.$$
$$\left. + w_3^{(n)}\delta(\mathbf{x} - \mathbf{x}_n)\delta(\xi - \xi_n)A_E\right], \tag{26}$$

where $C_N \equiv N/2$ is a normalization constant to ensure $\frac{1}{2}\int d\mathbf{x}\int_{-1}^{1}d\xi F_m(\mathbf{x}, \xi) = 1$ and δ is a Dirac delta function. The separation of the marker weight into the thermodynamic forces has been proposed by Tessarotto *et al.*[21] for gyrokinetic theory. We have applied this method to the monoenergetic drift-kinetic equation in Eq. (2) such that $(g - g_S A_E)/F_m = w_1 A_1 + w_3 A_3$. The monoenergetic transport coefficients D_{31} and D_{33} are therefore obtained from Eqs. (24) and (25). The numerical implementation of the present δf weighting scheme is discussed in Sec. III A.

The δf weighting scheme (26) involves the standard δf scheme to calculate the part corresponding to D_{31}. To see

this, we consider the standard one-weight δf scheme[11,22,23] based on Eq. (2), in which a marker weight $w \equiv g/F_m$ is given by

$$g(\mathbf{x}, \xi) = \frac{1}{C_N} \sum_{n=1}^{N} w^{(n)} \delta(\mathbf{x} - \mathbf{x}_n) \delta(\xi - \xi_n). \qquad (27)$$

The inner-product operation of $eBv\xi$ with g yields

$$\hat{j} \equiv e(Bv\xi, g) = -eD_{31}A_1 - eD_{33}A_E + \frac{e\langle B^2 \rangle v^2}{3\nu_D} A_E. \qquad (28)$$

In the calculation of the bootstrap current coefficient D_{31}, the parallel thermodynamic force is normally neglected, i.e., $A_E = 0$. Introducing the two marker weights w_1 and w_3, we can calculate D_{31} and D_{33} independently excluding a contribution from the Spitzer distribution for all collisionality regimes. When we apply the δf Monte Carlo method to the moment approach like that done with the DKES code, the latter feature becomes important for accurate evaluation of D_{33}.

C. Evaluation of the bootstrap current

Using the δf Monte Carlo method described above, the bootstrap current $\langle J_\parallel B \rangle$ can be evaluated with the moment approach. Here, we follow the formulation by Sugama and Nishimura.[12] We consider a plasma that consists of electrons and a single species of ions. In Secs. II A and II B, we have not specified particle species because under the pitch-angle scattering approximation, the monoenergetic transport coefficients depend only on the collisionality and are irrelevant to the particle species in these calculations. With the moment approach, nonetheless, the transport coefficients obtained as a function of ν_D/v can be used to describe the neoclassical transport for multispecies plasmas.[24]

To determine the bootstrap current, we need to solve the surface-averaged momentum and heat-flux balance equations for electrons and ions,

$$\langle \mathbf{B} \cdot (\nabla \cdot \boldsymbol{\pi}_a) \rangle - n_a e_a \langle BE_\parallel \rangle = \langle BF_{\parallel a1} \rangle, \qquad (29)$$

$$\langle \mathbf{B} \cdot (\nabla \cdot \boldsymbol{\Theta}_a) \rangle = \langle BF_{\parallel a2} \rangle. \qquad (30)$$

The neoclassical parallel viscosities $\langle \mathbf{B} \cdot (\nabla \cdot \boldsymbol{\pi}_a) \rangle$ and $\langle \mathbf{B} \cdot (\nabla \cdot \boldsymbol{\Theta}_a) \rangle$ in the left-hand side of Eqs. (29) and (30) are related to the plasma flows and the thermodynamic forces through the viscosity-flow relations

$$\begin{bmatrix} \langle \mathbf{B} \cdot (\nabla \cdot \boldsymbol{\pi}_a) \rangle \\ \langle \mathbf{B} \cdot (\nabla \cdot \boldsymbol{\Theta}_a) \rangle \end{bmatrix} = \begin{bmatrix} M_{a1} & M_{a2} \\ M_{a2} & M_{a3} \end{bmatrix} \begin{bmatrix} \langle u_{\parallel a} B \rangle / \langle B^2 \rangle \\ \frac{2}{5p_a} \langle q_{\parallel a} B \rangle / \langle B^2 \rangle \end{bmatrix} + \begin{bmatrix} N_{a1} & N_{a2} \\ N_{a2} & N_{a3} \end{bmatrix} \begin{bmatrix} X_{a1} \\ X_{a2} \end{bmatrix}, \qquad (31)$$

where

$$X_{a1} \equiv -\frac{1}{n_a} \frac{\partial p_a}{\partial s} - e_a \frac{\partial \Phi}{\partial s}, \qquad (32)$$

$$X_{a2} \equiv -\frac{\partial T_a}{\partial s}. \qquad (33)$$

Here, $\langle u_{\parallel a} B \rangle$ and $\langle q_{\parallel a} B \rangle$ are the surface-averaged flows of particles and heat, and $p_a = n_a T_a$ is the plasma pressure. The parallel friction forces $\langle BF_{\parallel a1} \rangle$ and $\langle BF_{\parallel a2} \rangle$ in the right-hand side of Eqs. (29) and (30) can also be expressed in terms of the coefficients l_{jk}^{ab} by the friction-force relations[16]

$$\begin{bmatrix} \langle BF_{\parallel a1} \rangle \\ \langle BF_{\parallel a2} \rangle \end{bmatrix} = \sum_b \begin{bmatrix} l_{11}^{ab} & -l_{12}^{ab} \\ -l_{21}^{ab} & l_{22}^{ab} \end{bmatrix} \begin{bmatrix} \langle Bu_{\parallel b} \rangle \\ \frac{2}{5p_a} \langle Bq_{\parallel b} \rangle \end{bmatrix}, \qquad (34)$$

which are valid in any toroidal geometry and in any collisionality regime. These friction-flow relations satisfy[16,25] the self-adjointness $l_{jk}^{ab} = l_{kj}^{ba}$ and the momentum conservation laws $\sum_a l_{1k}^{ab} = 0$. If one substitutes the viscosity-flow [Eq. (31)] and the friction-flow relations [Eq. (34)] into the parallel momentum and heat-flux balance equations [Eqs. (29) and (30)], the surface-averaged parallel current $\langle J_\parallel B \rangle$ is obtained by

$$\frac{\langle J_\parallel B \rangle}{\langle B^2 \rangle^{1/2}} = L_{E1}^e X_{e1} + L_{E2}^e X_{e2} + L_{E1}^i X_{i1} + L_{E2}^i X_{i2} + (L_{EE} + \sigma_S) X_E, \qquad (35)$$

where the linear transport coefficients L_{E1}^a and L_{E2}^a ($a = e, i$) are the (full energetic) electron and ion bootstrap current coefficients, L_{EE} is the neoclassical conductivity, and σ_S is the classical Spitzer conductivity. The parallel thermodynamic force X_E is defined as

$$X_E \equiv \frac{\langle BE_\parallel \rangle}{\langle B^2 \rangle^{1/2}}. \qquad (36)$$

Equation (35) determines the bootstrap current $\langle J_\parallel B \rangle$ locally on a flux surface for a given plasma profile in nonaxisymmetric devices.

Although the general expression of the friction-flow relations is obtained, the viscosity-flow relations must be specified by the solution of the drift-kinetic equation. Conventionally in nonaxisymmetric systems, the viscosity-flow relations have been obtained by the asymptotic expansion[8,25] of the drift-kinetic equation. In the present moment approach, this step is replaced by the δf Monte Carlo method. Following the moment approach by Sugama and Nishimura, we evaluate the two energy-dependent viscosity coefficients $M_a(K)$ and $N_a(K)$ in terms of the monoenergetic transport coefficients D_{31} and D_{33} as

$$M_a(K) = \frac{m_a^2}{T_a} [\nu_D^a(K)]^2 D_{33}(K) \times \left[1 - \frac{3m_a \nu_D^a(K) D_{33}(K)}{2T_a K \langle B^2 \rangle} \right]^{-1}, \qquad (37)$$

$$N_a(K) = \frac{m_a}{T_a} \nu_D^a(K) D_{31}(K) \left[1 - \frac{3m_a \nu_D^a(K) D_{33}(K)}{2T_a K \langle B^2 \rangle} \right]^{-1}.$$

(38)

The dependence of the bootstrap current on the magnetic configuration can be mainly determined by the viscosity coefficients $M_a(K)$ and $N_a(K)$. The neoclassical viscosity matrices M_{aj} and N_{aj} are given in the form of energy integrals as

$$[M_{aj}, N_{aj}] = n_a \frac{2}{\sqrt{\pi}} \int_0^\infty dK \sqrt{K} e^{-K} \left(K - \frac{5}{2} \right)^{j-1}$$

$$\times [M_a(K), N_a(K)].$$

(39)

The extension of the δf Monte Carlo method to the calculation of D_{33} enables us to evaluate $M_a(K)$ from Eq. (37). If we combine that with the results of D_{31}, we can also determine the other coefficient $N_a(K)$ using Eq. (38). The δf Monte Carlo method does not rely on the asymptotic expansion of the drift-kinetic equation. The viscosity-flow relations can be determined for arbitrary collisionality similar to the DKES code. Because the neoclassical viscosity is dominated by the test-particle portion of the collision operator,[16] the use of the pitch-angle scattering operator without the momentum conservation is justified to calculate the neoclassical viscosity.[12] Because of the conservation properties of the friction-flow relations in Eq. (34), the bootstrap current $\langle J_\| B \rangle$ can be calculated appropriately with the moment equations. An algebraic procedure to solve the moment equations is given in Ref. 12.

III. NUMERICAL TESTS

In this section, we verify the numerical calculation of D_{33} and of the viscosity coefficients M and N using the δf Monte Carlo method. As already mentioned, these calculations account for the main portion of the present moment approach. As a δf Monte Carlo code, we here used the VENUS+δf code,[9] which has been used[7,9,26] to calculate the bootstrap current coefficient D_{31} for several nonaxisymmetric devices. We have implemented the δf weighting scheme described in Sec. II B into this code for calculating D_{33}.

We carried out calculation in a magnetic field model of LHD, where the poloidal and toroidal-field periods are $l=2$ and $m=10$. The field strength in Boozer coordinates is given by

$$B = B_0[1 - \epsilon_t(r)\cos\theta - \epsilon_h(r)\cos(l\theta - m\zeta)],$$

(40)

where the average minor radius r is chosen as a flux surface label. The toroidal geometry is specified by those values of major radius $R=4$ m, the minor radius of last closed flux surface $a=0.8$ m, and $B_0=1$ T. The rotational transform is assumed to be radially constant as $\iota=0.375$. The effect of the net toroidal current on the equilibrium is neglected. We set the radial profile of magnetic field ripple by $\epsilon_t = \epsilon_{ta}(r/a)$ and $\epsilon_h = \epsilon_{ha}(r/a)^2$, where ϵ_{ta} and ϵ_{ha} are the values at the last closed flux surface. In the following calculations, the test particles were started from the initial surface: $r/a=0.5$
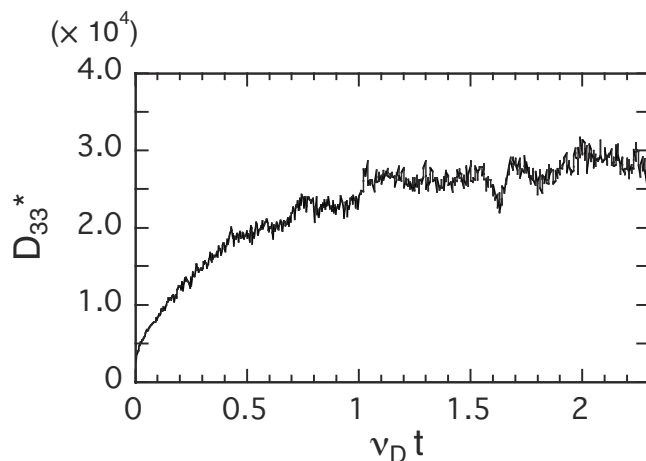

FIG. 1. A typical time history of the normalized coefficient $D_{33}^* \equiv D_{33}/(\frac{1}{2}v_T K^{1/2})$ calculated with the VENUS+δf code for $\epsilon_t=0.1$ and $\epsilon_h=0.05$. The collisionality is in the banana regime ($\nu_D/v=1\times10^{-5}$).

at time $t=0$. Thus we denote $\epsilon_t(r)$ and $\epsilon_h(r)$ by values on $r/a=0.5$.

A. The δf Monte Carlo code

The numerical procedure of the VENUS+δf code is briefly summarized as follows. A three-dimensional magnetohydrodynamic (MHD) equilibrium described in Boozer coordinates is given as input data. The guiding-center trajectories of test particles are obtained from the drift orbit equations, which are solved with the Runge–Kutta schemes of second and fourth orders with fixed time steps.[27] At each time step, the pitch-angle scattering is simulated by the Monte Carlo collision operator,[28] and the perturbed distribution function δf is updated by the radial excursions of test particles. In the original code, the monoenergetic bootstrap current, which is here denoted by $\hat{j}_{bs}$, is calculated by the standard one-weight δf scheme with $A_E \equiv 0$.

To extend the δf weighting scheme used in the VENUS+δf code, we have implemented the marker weight $w_3 \equiv g_3/F_m$ with the weight equation of Eq. (22) into the code, which allows us to evaluate D_{33} by the Monte Carlo integral of Eq. (25). The weight equation [Eq. (22)] for D_{33} is explicitly written in Boozer coordinates as

$$\frac{Dw_3}{Dt} = -\frac{v^2}{\nu_D} P_2(\xi) \left(\frac{\psi'}{\mathcal{J}_B} \frac{\partial}{\partial \zeta} + \frac{\chi'}{\mathcal{J}_B} \frac{\partial}{\partial \theta} \right) \ln B,$$

(41)

where the prime denotes derivative with respect to the flux surface label, ψ is the toroidal flux, and χ is the poloidal flux. Figure 1 shows the typical time evolution of D_{33}. The simulation reached the steady state in several collision times, and a value of D_{33} was calculated from the time averaging over a finite interval of this steady state. To check the convergence, the Monte Carlo noise ΔD_{33} is measured with respect to this time averaging. We should note that Eq. (23) does not include the nonlinear drift-term $\mathbf{v}_d \cdot \nabla$, which implies that the Lagrangian derivative D/Dt represents the derivative along the equilibrium trajectories.[11] A simple way to realize such a test-particle trajectory in the simulation is to choose particle velocities small enough such that ρ_p/a remains much smaller
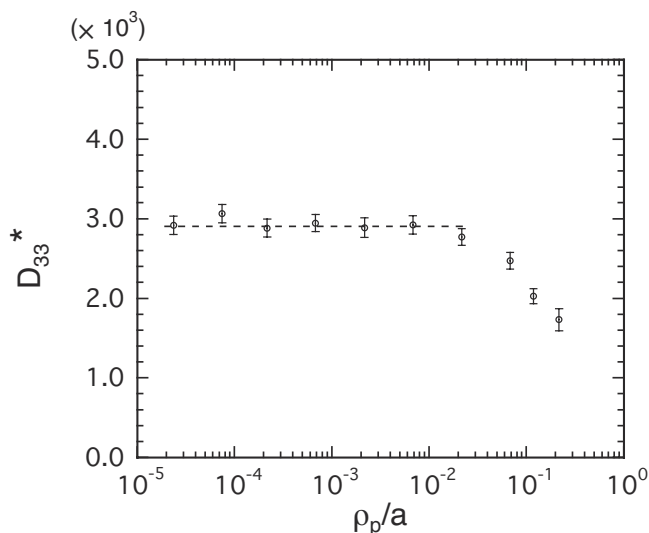
FIG. 2. The normalized coefficient $D_{33}^*=D_{33}/(\frac{1}{2}v_T K^{1/2})$ vs ρ_p/a calculated with the VENUS+δf code for $\epsilon_t=0.1$ and $\epsilon_h=0.05$. The collisionality is in the banana regime ($\nu_D/v=1\times10^{-4}$).

FIG. 3. The normalized coefficient $D_{33}^*\equiv D_{33}/(\frac{1}{2}v_T K^{1/2})$ vs ν_D/v calculated with the VENUS+δf code for $\epsilon_t=0.1$ and $\epsilon_h=0$. The solid line shows the asymptotic values in the banana regime.

than unity in all collisionalities. Under this condition, the transport coefficients become insensitive to this parameter. Figure 2 shows the ρ_p/a dependence of transport coefficients D_{33} obtained by the code. In Fig. 2 and in the following, the diagonal elements D_{33} are normalized as $D_{33}^*\equiv D_{33}/(\frac{1}{2}v_T K^{1/2})$. For small ρ_p/a ($<10^{-2}$), D_{33}^* is not sensitive to this dimensionless parameter and for large ρ_p/a, the D_{33}^* decreases with ρ_p/a. In the latter case, test particles deviate from the initial surface owing to the radial guiding-center drifts. In the following calculations, we chose $\rho_p/a\simeq4\times10^{-4}$ to ensure negligible finite-orbit width effects.

In the simulation, we used $N\gtrsim10^4$ particles. As already mentioned, an important feature of the moment approach is to calculate the neoclassical viscosity for arbitrary collisionality. To keep this feature, we require the accurate calculation of D_{33} for a wide range of collision frequencies. To assist this, we used a supplementary method to improve the numerical convergence of D_{33} in the collisional regime: typically for $\nu_D/v\gtrsim10^{-2}$. This method will be discussed in the Appendix, and it was utilized to obtain the numerical results in this paper.

B. Numerical results

We illustrate the numerical results for a model field defined in the beginning of this section. For comparison, we carried out calculations for the same parameters with those used in Ref. 12 and compared the numerical results obtained by the VENUS+δf code with those obtained by the DKES code, where the results of the latter are given in Ref. 12. Figure 3 shows the collisionality dependence of the calculated D_{33}^* in the axisymmetric limit, $\epsilon_h=0$. The solid line shows the asymptotic formula[13] in the banana regime for D_{33}^*,
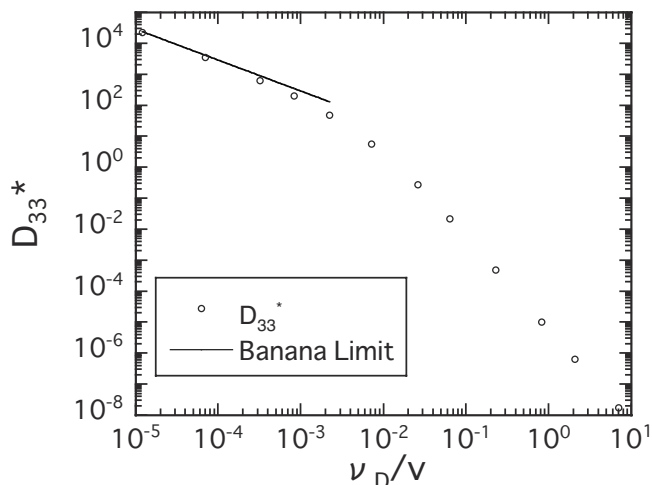
$$D_{33}^* = f_t\langle B^2\rangle\frac{2}{3(\nu_D/v)}. \tag{42}$$

We thus confirmed the good convergence of D_{33}^* in this regime. Figure 4 shows the results for several values of ϵ_h such that $\epsilon_h=0$, 0.01, 0.05, and 0.1, where ϵ_t in Eq. (40) is kept constant as $\epsilon_t=0.1$. The difference due to the amplitude of helical ripple ϵ_h manifests itself mainly in the plateau and the collisional regimes. The results in Fig. 4 show good agreement with those in Ref. 12.

Using the results of Fig. 4, we calculate the energy-dependent viscosity coefficients $M(K)$ and $N(K)$. First, Fig. 5 shows the ϵ_h dependence of a normalized viscosity coefficient M^*, where $M^*\equiv M(K)/(mv_T K^{3/2})$. The viscosity coefficient $M(K)$ measures the damping rate of neoclassical flows along the field line. The normalized coefficient M^* is written in terms of the normalized coefficient D_{33}^* as
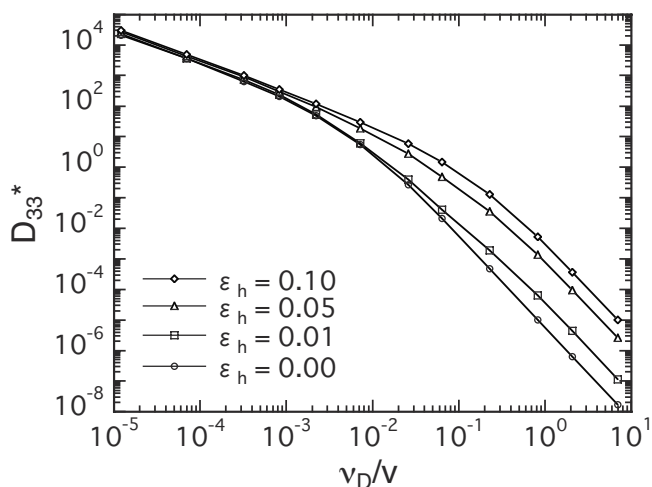

FIG. 4. The normalized coefficient $D_{33}^*\equiv D_{33}/(\frac{1}{2}v_T K^{1/2})$ vs ν_D/v calculated with the VENUS+δf code for $\epsilon_h=0$, 0.01, 0.05, and 0.1 with $\epsilon_t=0.1$.
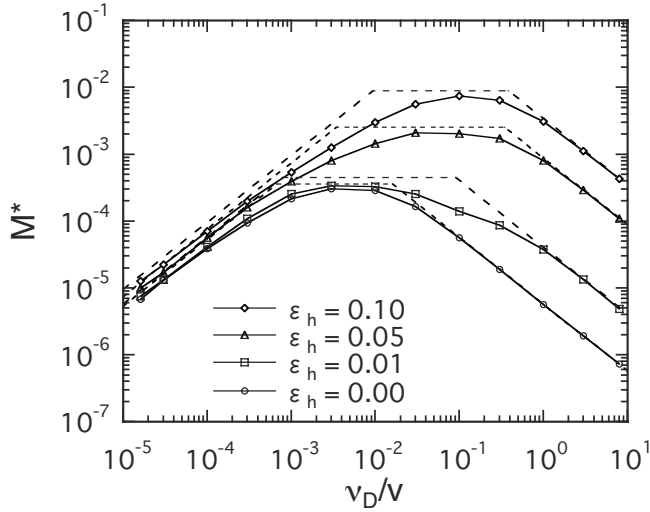
FIG. 5. The normalized viscosity coefficient $M^* \equiv M(K)/(mv_T K^{3/2})$ vs ν_D/v calculated with the VENUS+δf code. The dashed segments show the asymptotic values of M^* for the three collisionality regimes.

$$M^* = \frac{(\nu_D/v)^2 D_{33}^*}{1 - \frac{3}{2}(\nu_D/v)D_{33}^*/\langle B^2\rangle}. \tag{43}$$

The dashed segments in Fig. 5 show the asymptotic values in the Pfirsch–Schlüter, plateau, and banana regimes. The asymptotic formulae used here are given by[12]

$$M_{\text{P.S.}}^* = \frac{2}{5}\langle(\mathbf{B}\cdot\nabla\ln B)^2\rangle[\nu_T(K)/v]^{-1}, \tag{44}$$

$$M_{\text{plateau}}^* = \frac{\pi}{4}\langle B^2\rangle^{1/2}(4\pi^2/V')$$
$$\times\left(\sum_{(m,n)\neq(0,0)}|\beta_{mn}|^2|m\chi' - n\psi'|\right), \tag{45}$$

$$M_{\text{banana}}^* = \frac{2}{3}(f_t/f_c)\langle B^2\rangle[\nu_D(K)/v], \tag{46}$$

where V is the volume enclosed by the flux surface and β_{mn} is the magnetic-field spectrum in Hamada coordinates.[29] The ratio of the fraction of trapped particles to that of circulating ones is denoted by f_t/f_c. To be consistent with Ref. 12, the test-particle frequency ν_T in Eq. (44) is set as $\nu_T = 3\nu_D$. In Fig. 5, the results obtained from the δf Monte Carlo method are in reasonable agreement with the asymptotic formulae. Next, we calculate the ϵ_h dependence of a normalized viscosity coefficient $N(K)^*$, where $N^* \equiv N(K)/[(Bv_T/\Omega)K^{3/2}]$. The viscosity coefficient $N(K)$ measures the driving force of parallel flows mainly due to the trapped particles. The normalized coefficient N^* is written in terms of D_{31}^* and D_{33}^* as

$$N^* = \frac{(\nu_D/v)D_{31}^*}{1 - \frac{3}{2}(\nu_D/v)D_{33}^*/\langle B^2\rangle}, \tag{47}$$

where the bootstrap current coefficient D_{31} is normalized as $D_{31}^* \equiv D_{31}/\left[\frac{1}{2}v_T(Bv_T/\Omega)K\right]$. Figure 6 shows the results for N^*. Also plotted for benchmarking are the results[12] obtained from the DKES code. The δf Monte Carlo method has reproduced the curve obtained by the DKES code. Consequently, the numerical results for $M(K)$ and $N(K)$ obtained
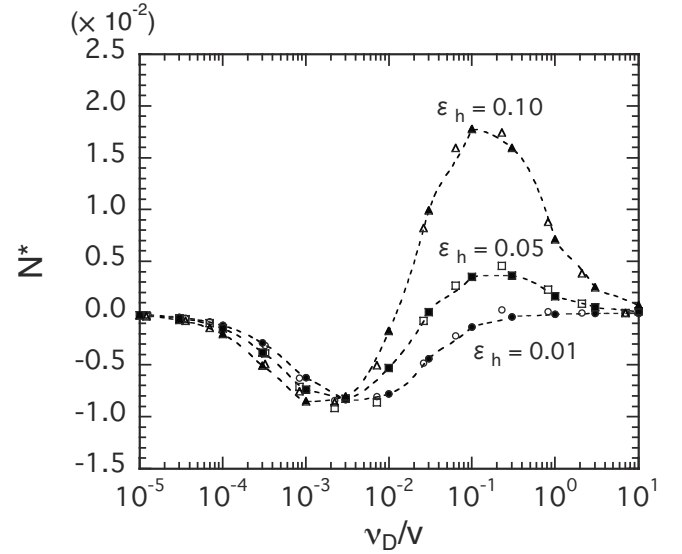

FIG. 6. The normalized viscosity coefficient $N^* \equiv N(K)/[(Bv_T/\Omega)K^{3/2}]$ vs ν_D/v. The open symbols show the numerical results from the VENUS+δf and the closed symbols show those from the DKES code in Ref. 12.

here are in reasonable agreement with the asymptotic formulae and with those obtained by the DKES code. We thus conclude that these numerical tests provide a sufficient basis for applying the δf Monte Carlo method to the moment approach.

IV. CONCLUSION

A δf Monte Carlo method has been presented to evaluate the bootstrap current in nonaxisymmetric toroidal plasmas with the moment approach. Using the δf weighting scheme proposed in this work, the diagonal (D_{33}) and the nondiagonal (D_{31}) elements of the monoenergetic transport matrix are calculated. The former have been calculated so far only by the variational principle. In the numerical tests, we have calculated the energy-dependent viscosity coefficients M and N from D_{31} and D_{33} and have obtained the reasonable agreement between the variational principle and the asymptotic formulae. With the moment approach, the bootstrap current $\langle J_\parallel B\rangle$ is evaluated from these viscosity coefficients with the algebraic moment equations that satisfy the physical requirement of the conservation laws.

We have implemented the above δf weighting scheme into one of δf Monte Carlo codes, namely, the VENUS+δf. This code has been applied to the calculation of D_{31} in several nonaxisymmetric devices such as LHD.[26] In the LHD experiment, the time evolution of the bootstrap current profiles has recently become possible to be measured.[30] The present work will be useful for experimental analysis of the bootstrap current in LHD as future applications.

APPENDIX: CALCULATION OF D_{33} IN COLLISIONAL REGIME

In this appendix, we discuss an additional topic of the δf Monte Carlo method to calculate D_{33}. The subject addressed here is about the expression for the calculation of D_{ij} in the variational principle, which is given by Eq. (7). In this equation, the time-reversal flux[14] $\sigma_i^+ (i=1,3)$ is used not only for the source term of the drift-kinetic equation but for the integrand in the inner-product operation as well. We found that a similar expression for the δf Monte Carlo method was useful to improve the numerical convergence of D_{33} in the collisional regime.

To derive an expression of D_{33} like Eq. (7), we use the symmetric properties of the operators $V_\parallel$ and C in Eq. (12). In Eq. (18), D_{33} is given by $D_{33}=-(Bv\xi,g_3)$. Using the symmetric properties of Eq. (12),

$$D_{33} = -(Bv\xi,g_3) = (C(Bv\xi/\nu_D),g_3) = (Bv\xi/\nu_D,Cg_3)$$

$$= (Bv\xi/\nu_D,V_\parallel g_3) + (Bv\xi/\nu_D,\sigma_3^+) = -(\sigma_3^+,g_3), \qquad (A1)$$

where $(Bv\xi/\nu_D,\sigma_3^+)$ automatically vanishes. Note that ξ is the eigenfunction of the pitch-angle scattering operator $\nu_D^{-1}C$ with the eigenvalue of -1. Therefore, $C(Bv\xi/\nu_D)=-Bv\xi$. From Eq. (A1), we have obtained another expression for D_{33},

$$D_{33} = -\left(\sigma_3^+,g_3(\mathbf{x},\xi)\right) = -\frac{\sum_{n=1}^N \mathcal{J}_B(\mathbf{x}_n)\sigma_3^+(\mathbf{x}_n,\xi_n)w_3^{(n)}}{\sum_{n=1}^N \mathcal{J}_B(\mathbf{x}_n)}. \qquad (A2)$$

The physical meaning of the equivalence between Eqs. (25) and (A2) can be seen by taking the inner product of Eq. (19) with $Bv\xi$,

$$(Bv\xi,V_\parallel g_3) - (Bv\xi,Cg_3) = 0. \qquad (A3)$$

From Eqs. (A1) and (A3), we see that $(Bv\xi,g_3)$ is proportional to the momentum lost by collisions; (σ_3^+,g_3) is proportional to the momentum generated indirectly by the trapped particles. From these physical pictures, we understand that the numerical values $(Bv\xi,g_3)$ and (σ_3^+,g_3) measure the quantities that are in balance with each other. In actual simulations, however, such an exact balance cannot be achieved because the terms (σ_3^+,g_3) and $(Bv\xi,g_3)$ are characterized by the different relaxation times in transient phase of a initial-value problem. To obtain the results in Sec. III B, we attempted the calculation of D_{33} using both terms and consequently found that the calculated transport coefficients experience different levels of the Monte Carlo noise. Figure 7 shows the collisionality dependence of the noise observed for D_{33} in the nonaxisymmetric case with $\epsilon_h=0.05$. In the low collisionality regime of $\nu_D \lesssim 10^{-2}$, the noise for $D_{33}\equiv-(\sigma_3^+,g_3)$ is considerably larger than that of $D_{33}=-(Bv\xi,g_3)$. In contrast, we obtained good convergence
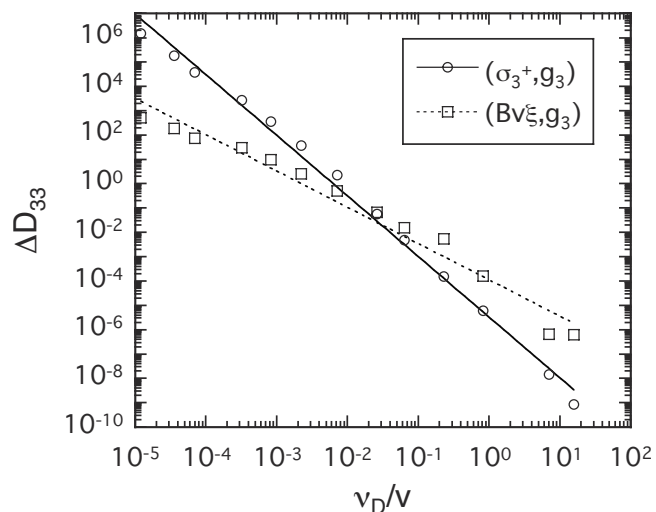

FIG. 7. The absolute values of the Monte Carlo noise denoted by ΔD_{33} vs ν_D/v for two different expressions for D_{33} in Eqs. (25) and (A2). Here, $\epsilon_t=0.1$ and $\epsilon_h=0.05$. The number of test particles is $N \gtrsim 10^4$ for all points. (The same number of test particles was used for each ν_D/v.)

of D_{33} by the expression $D_{33}=-(\sigma_3^+,g_3)$ for the collisional regime with $\nu_D \gtrsim 10^{-2}$. This result suggests that the use of Eq. (A2) is favorable in the collisional regime to improve the statistical convergence of D_{33}. This result can be interpreted by the difference of relaxation times between (σ_3^+,g_3) and $(Bv\xi,g_3)$.

Finally, we note that the bootstrap current D_{31} can also be calculated by $D_{31}=-(\sigma_3^+,g_1)$ in a similar way to Eq. (A2). Moreover, we see from the Onsager relation that the Ware flux coefficient D_{13} can also be used as a measure of the nondiagonal elements of transport matrix; the Ware flux coefficient D_{13} can be calculated using the marker weight w_3 introduced in this paper. Such arbitrariness of the expression to calculate the monoenergetic transport coefficients is a freedom that may be used to improve statistics in the δf Monte Carlo methods.

[1] K. C. Shaing, E. C. Crume, Jr., J. S. Tolliver, S. P. Hirshman, and W. I. van Rij, Phys. Fluids B **1**, 148 (1989).
[2] K. C. Shaing, B. A. Carreras, N. Dominguez, V. E. Lynch, and J. S. Tolliver, Phys. Fluids B **1**, 1663 (1989).
[3] K. Y. Watanabe, N. Nakajima, M. Okamoto, K. Yamazaki, Y. Nakamura, and M. Wakatani, Nucl. Fusion **35**, 335 (1995).
[4] W. A. Cooper, S. F. Margalet, S. J. Allfrey, M. Yu. Isaev, M. I. Mikhailov, V. D. Shafranov, A. A. Subbotin, Y. Narushima, S. Okamura, C. Suzuki, K. Yamazaki, G. Y. Fu, L. P. Ku, D. A. Monticello, M. H. Redi, A. H. Reiman, M. C. Zarnstorff, J. Nührenberg, and T. N. Todd, Plasma Phys. Controlled Fusion **44**, B357 (2002).
[5] A. H. Boozer and H. J. Gardner, Phys. Fluids B **2**, 2408 (1990).
[6] Y. Wu and R. B. White, Phys. Fluids B **5**, 3291 (1993).
[7] K. Allmaier, C. D. Beidler, M. Yu. Isaev, S. V. Kasilov, W. Kernbichler, H. Maassberg, S. Murakami, D. A. Spong, and V. Tribaldos, in 16th International Stellarator/Heliotron Workshop, Toki, 2007, edited by S. Morita (National Institute for Fusion Science, Toki, 2008), pp. P2–029.
[8] K. C. Shaing and J. D. Callen, Phys. Fluids **26**, 3315 (1983).
[9] M. Yu. Isaev, S. Brunner, W. A. Cooper, T. M. Tran, A. Bergmann, C. D. Beidler, J. Geiger, H. Maassberg, J. Nührenberg, and M. Schmidt, Fusion Sci. Technol. **50**, 440 (2006).
[10] K. Allmaier, S. V. Kasilov, W. Kernbichler, and G. O. Leitold, Phys. Plasmas **15**, 072512 (2008).
[11] Z. Lin, W. M. Tang, and W. W. Lee, Phys. Plasmas **2**, 2975 (1995).
[12] H. Sugama and S. Nishimura, Phys. Plasmas **9**, 4637 (2002).

[13] H. Sugama and S. Nishimura, Phys. Plasmas **15**, 042502 (2008).

[14] S. P. Hirshman, K. C. Shaing, W. I. van Rij, C. O. Beasely, Jr., and E. C. Crume, Jr., Phys. Fluids **29**, 2951 (1986).

[15] W. I. van Rij and S. P. Hirshman, Phys. Fluids B **1**, 563 (1989).

[16] S. P. Hirshman and D. J. Sigmar, Nucl. Fusion **21**, 1079 (1981).

[17] M. Taguchi, Phys. Fluids B **4**, 3638 (1992).

[18] O. Motojima, H. Yamada, A. Komori, N. Ohyabu, K. Kawahata, O. Kaneko, S. Masuzaki, A. Ejiri, M. Emoto, H. Funaba, M. Goto, K. Ida, H. Idei, S. Inagaki, N. Inoue, S. Kado, S. Kubo, R. Kumazawa, T. Minami, J. Miyazawa, T. Morisaki, S. Morita, S. Murakami, S. Muto, T. Mutoh, Y. Nagayama, Y. Nakamura, H. Nakanishi, K. Narihara, K. Nishimura, N. Noda, T. Kobuchi, S. Ohdachi, Y. Oka, M. Osakabe, T. Ozaki, B. J. Peterson, A. Sagara, S. Sakakibara, R. Sakamoto, H. Sasao, M. Sasao, K. Sato, M. Sato, T. Seki, T. Shimozuma, M. Shoji, H. Suzuki, Y. Takeiri, K. Tanaka, K. Toi, T. Tokuzawa, K. Tsumori, K. Tsuzuki, I. Yamada, S. Yamaguchi, M. Yokoyama, K. Y. Watanabe, T. Watari, Y. Hamada, K. Matsuoka, K. Murai, K. Ohkubo, I. Ohtake, M. Okamoto, S. Satoh, T. Satow, S. Sudo, S. Tanahashi, K. Yamazaki, M. Fujiwara, and A. Iiyoshi, Phys. Plasmas **6**, 1843 (1999).

[19] A. H. Boozer, Phys. Fluids **26**, 1288 (1983).

[20] A. Y. Aydemir, Phys. Plasmas **1**, 822 (1994).

[21] M. Tessarotto, R. B. White, and L. J. Zheng, Phys. Plasmas **1**, 2603 (1994).

[22] M. Sasinowski and A. H. Boozer, Phys. Plasmas **2**, 610 (1995).

[23] K. Hanatani, J. Plasma Fusion Res. Series **1**, 472 (1998).

[24] S. Nishimura, H. Sugama, and CHS Group, Fusion Sci. Technol. **46**, 77 (2004).

[25] N. Nakajima and M. Okamoto, J. Phys. Soc. Jpn. **61**, 833 (1992).

[26] M. Yu. Isaev, K. Y. Watanabe, M. Yokoyama, N. Ohyabu, C. D. Beidler, H. Maassberg, W. A. Cooper, T. M. Tran, and M. I. Mikhailov, Plasma Fusion Res. **3**, 036 (2008).

[27] O. Fischer, W. A. Cooper, M. Yu. Isaev, and L. Villard, Nucl. Fusion **42**, 817 (2002).

[28] A. H. Boozer and G. Kuo-Petravic, Phys. Fluids **24**, 851 (1981).

[29] S. Hamada, Nucl. Fusion **2**, 23 (1962).

[30] Y. Nakamura, K. Y. Watanabe, K. Kawaoto, K. Ida, Y. Narushima, M. Yoshinuma, S. Sakakibara, I. Yamada, T. Tokuzawa, M. Goto, K. Tanaka, N. Nakajima, K. Kawahata, and LHD Experimental Group, in *Proceedings of the 22nd Fusion Energy Conference* (IAEA, Geneva, Switzerland, 2008), pp. EX/P6–20.